Tree Physiology 00, 1–16
doi:10.1093/treephys/tpaa120

Research paper

Responses of functional traits to seven-year nitrogen addition in two tree species: coordination of hydraulics, gas exchange and carbon reserves

Hongxia Zhang[1,4], Fenghui Yuan[1], Jiabing Wu[1], Changjie Jin[1], Alexandria L. Pivovaroff[2], Jinyuan Tian[1,4], Weibin Li[3], Dexin Guan[1,6], Anzhi Wang[1,6] and Nate G. McDowell[2,5]

[1]Key Laboratory of Forest Ecology and Management, Institute of Applied Ecology, Chinese Academy of Sciences, Shenyang 110016, China; [2]Atmospheric Sciences & Global Change Division, Pacific Northwest National Laboratory, Richland, WA 99354, USA; [3]State Key Laboratory of Grassland and Agro-ecosystems, Key Laboratory of Grassland Livestock Industry Innovation, Ministry of Agriculture and Rural Affairs, College of Pastoral Agriculture Science and Technology, Lanzhou University, Lanzhou 730020, China; [4]University of Chinese Academy of Sciences, Beijing 100049, China; [5]School of Biological Sciences, Washington State University, Pullman, WA 99164-4236, USA; [6]Corresponding authors D. Guan (dxguan@iae.ac.cn); A. Wang (waz@iae.ac.cn)

Received January 1, 2020; Revised July 25, 2020; accepted September 16, 2020; handling Editor David Tissue

Atmospheric nitrogen (N) deposition has been observed to impact plant structure and functional traits in terrestrial ecosystems. Although the effect of N deposition on plant water use has been well-evaluated in laboratories and in experimental forests, the linkages between water and carbon relations under N deposition are unclear. Here, we report on hydraulics, gas exchange and carbon reserves of two broad-leaved tree species (*Quercus mongolica* and *Fraxinus mandshurica*) in mature temperate forests after a seven-year experiment with different levels of N addition (control (CK), low (23 kg N ha^{-1} yr^{-1}), medium (46 kg N ha^{-1} yr^{-1}) and high (69 kg N ha^{-1} yr^{-1})). We investigated variation in hydraulic traits (xylem-specific hydraulic conductivity (K_s), native percentage loss of conductivity (*PLC*) and leaf water potential), xylem anatomy (vessel diameter and density), gas exchange (maximum net photosynthesis rate and stomatal conductance) and carbon reserves (soluble sugars, starch and total nonstructural carbohydrates (*NSC*)) with different N addition levels. We found that medium N addition significantly increased K_s and vessel diameter compared to control, but accompanied increasing *PLC* and decreasing leaf water potential, suggesting that N addition results in a greater hydraulic efficiency and higher risk of embolism. N addition promoted photosynthetic capacity via increasing foliar N concentration but did not change stomatal conductance. In addition, we found increase in foliar soluble sugar concentration and decrease in starch concentration with N addition, and positive correlations between hydraulic traits (vessel diameter and *PLC*) and soluble sugars. These coupled responses of tree hydraulics and carbon metabolism are consistent with a regulatory role of carbohydrates in maintaining hydraulic integrity. Our study provides an important insight into the relationship of plant water transport and carbon dynamics under increasing N deposition.

Keywords: hydraulic architecture, hydraulic conductivity, nitrogen fertilization, nonstructural carbohydrates, photosynthetic rate, vessel diameter.

Introduction

Atmospheric nitrogen (N) deposition has increased by threefold to fivefold due to fossil combustion and artificial fertilizer application over the past century (IPCC 2007; Galloway et al. 2008), and is predicted to continue increasing by a factor of 2.5 by the end of the century (Davidson 2009, Fowler et al. 2013). Increased soil N availability can enhance forest photosynthesis and water-use efficiency (Magill et al. 2004, Hoegberg et al. 2006, Li et al. 2015, Zhang et al. 2018), and subsequently increasing forest productivity (Lovelock et al. 2004, Leonardi et al. 2012, Keenan et al. 2013). However, long-term increases in N deposition will eventually rise to excessive levels and may trigger ion/nutrient imbalance in plants, which would potentially exacerbate vegetation vulnerability to stressors and are expected to overwhelm the benefits mentioned above (Van de Weg et al. 2013, Borghetti et al. 2017). Yet the physiological mechanism by which long-term N deposition affects vegetation to climate changes is currently unknown.

High N availability can cause changes in plant leaf economics, gas exchange and hydraulic traits (Hacke et al. 2010, Villagra et al. 2013, Zhang et al. 2018). For example, N addition can increase foliar N content and leaf area, thereby enhancing leaf-level photosynthesis and gas exchange (Evans 1989, Grassi et al. 2002). Likewise, high N nutrition can affect whole-plant hydraulic conductance through altering plant xylem hydraulic architecture (e.g., conduit diameter and density; Goldstein et al. 2013, Pivovaroff et al. 2016, Fang et al. 2017, Mozdzer and Caplan 2018), which is a proxy of hydraulic function (Bucci et al. 2006, Fonti et al. 2010, Plavcová and Hacke 2012, Goldstein et al. 2013). Previous N-addition experiments have revealed that high N conditions increased the diameter of xylem conduits (Harvey and van den Driessche 1999, Plavcová and Hacke 2012, Goldstein et al. 2013), which likely enhances specific conductivity (e.g., the efficiency of water transport; Bucci et al. 2006, Hacke et al. 2010, Goldstein et al. 2013). However, wider xylem conduits are also more likely to experience the prevailing environmental stress (e.g., freeze–thaw embolism; Davis et al. 1999, Pittermann and Sperry 2003, Niu et al. 2017), meaning that the efficient xylem conductivity comes at the cost of being more vulnerable to hydraulic failure (Hacke et al. 2006). Recent research supports this pattern (Goldstein et al. 2013, Plavcová et al. 2013), but the trade-offs of the relationship between the efficiency and the safety under N deposition remain unclear.

Hydraulic function is interdependent with carbohydrate utilization processes (McDowell 2011, Anderegg and Anderegg 2013). Stored nonstructural carbohydrate concentrations (*NSC*) buffer asynchrony of substrate supply and demand and thus mitigate mortality risk under environmental stresses (i.e., drought). Nonstructural carbohydrate concentrations also play a critical role in regulating hydraulic function through maintaining tissue water potential through their role as osmolytes (Galiano et al. 2011, Sala et al. 2012, O'Brien et al. 2014, Hartmann and Trumbore 2016, Adams et al. 2017). Previous synthesis results indicated that N enrichment significantly increased *NSC* comsuption via growth and respiration and hence decreased *NSC* storage in plants (particualy in foliage and roots; Li et al. 2018, 2020), the extra xylem growth of which may influence plant architecture toward altered hydraulic efficiency and/or safety (Magnani et al. 2002, Sack et al. 2003, Mcdowell 2011, Fatichi et al. 2014). Specifically, enhanced growth of xylem tissues under N addition could alter xylem structure (e.g., wider diameter), subsequently impacting hydraulic efficiency and safety. In addition, *NSC* reserves in plant tissues can adjust osmotic pressure and water potential, which could help to maintain a water potential gradient between leaves and soil (Clifford et al. 1998, Mitchell et al. 2014). Besides these metabolic processes and osmotic adjustment (Dichio et al. 2009), previous results suggested that soluble sugar (one of main components of *NSC*) can be used in energy-driven refilling of embolized vessels under negative pressure for embolism repair (Holbrook et al. 1999, Hacke and Sperry 2003, Nardini et al. 2011, Secchi and Zwieniecki 2011), and generated root or stem pressure may partially free some temperate tree species from freeze-induced embolism (Niu et al. 2017). The embolism repair process relies on generation of local positive pressures via osmotic mechanisms triggered by soluble release from vessel-associated parenchyma into the embolized conduit, although underlying mechanisms remain unclear (Salleo et al. 2004, Secchi and Zwieniecki 2012). Hence, understanding the coordination of plant hydraulic-carbon strategies to prolong survival with atmospheric N deposition is necessary.

In the present study, current-year branch xylem hydraulic conductivity, water potential, native *PLC*, associated xylem structural characteristics, gas exchange, leaf carbon/nitrogen (C/N) ratio and *NSC* were investigated in two main temperate broad-leaved species. Our objectives were to identify the responses of hydraulics, gas exchange and carbon reserves to seven-year N addition, and investigate the relationships among these functional traits. We hypothesized that: (1) N addition will shift hydraulic architecture such that it results in higher hydraulic conductivity, but also result in higher *PLC*, (2) gas exchange will be enhanced by increasing foliar N concentration under N addition and (3) *NSC* concentrations will be reduced due to increased consumption under N addition.

Materials and method

Field site description

The study was conducted at the Research Station of Changbai Mountain Forest Ecosystems of the Chinese Academy of Sciences (128°28′E, 42°24′N; 738 m altitude), which is located in Jilin province, NE China. The site has a temperate continental climate with long and cold winters and relatively short and

cool summers. Mean annual temperature in 2017 was 4.0 °C and monthly range fluctuating from −13.6 to 20.8 °C. The mean annual temperature is approximately 4.1 °C across nearly 36 years (Meteorological data from the Research Station of Changbai Mountain Forest Ecosystems of the Chinese Academy of Sciences; Figure S2 available as Supplementary Data at *Tree Physiology* Online). The highest summer temperature often occurs in July or August, averaging 16.2 °C throughout the study period (May to September). Mean annual precipitation was 650.8 mm (Figure S2 available as Supplementary Data at *Tree Physiology* Online) during the study period and was strongly influenced by the summer monsoon with ~60–70% occurring from June to September. The soil is montane dark brown soil developed from volcanic ash (Albi-Boric Argosols). The study site was established in a flat area, with the slope ranging from 1° to 5°. The area is covered with 300-year-old mixed forests of oak, pine and ash, interspersed with larch and mono maple. The mean canopy height is about 27 m and the stand density is 560 stems ha^{-1} (stem diameter > 8 cm; Li et al. 2017).

Experimental design and plant material

N addition treatments were carried out from 2011 to 2017, following a randomized complete block design. The urea was divided into five equal doses and sprayed to the plots from May to September each year at four different rates (0, 23, 46 and 69 kg N ha^{-1} yr^{-1}). Each plot is 15 m × 15 m, which was separated by 5 m buffer area. Hence, there were four treatments in total, with each treatment present in each of the four blocks (thus four replicates of each treatment). *Quercus mongolica* (simple-leaved species) and *Fraxinus mandshurica* (compound-leaved species) were selected for the present study, which are the typical angiosperm tree species in the mixed forest of this region. One or two trees of each target species (*Quercus mongolica* and *Fraxinus mandshurica*) with tree height in each plot were identified as target trees. The target trees were always located near the plot center. The average tree height of the selected trees was 25 m and all samples were collected in sun-exposed crowns from selected trees at canopy positions 15–18 m in height.

Leaf water potential and xylem hydraulic conductivity

In August 2017, we randomly collected one branch (~1.5 m in length; on the sun-exposed crown) of each target species from separate individuals in each plot in the morning. In other words, four treatments × four replicates (four plots per treatment) × two species equaled a total of 32 branches collected from all plots in the same morning. The cut ends were covered with parafilm and samples were placed in large opaque plastic bags with wet towels to prevent the samples from drying out, then transported to the laboratory immediately (the study site is about 10 min driving from the Research Station). Leaves were cut from the branches before measuring hydraulic conductivity and immediately sealed in plastic bags containing a moist towel and kept in a cooler until balancing pressures were determined in the laboratory at the research station within 1 h of sample collection. Leaf water potential (Ψ_L) was measured with a pressure chamber (Model 1505D, PMS Instrument Company, USA) on six to eight of the newest fully developed mature leaves for each N addition treatment. Branches were immediately recut (~5 cm removed) under water to remove embolized vessels. Current-year branches used for hydraulic conductivity measurements had the cut end covered with parafilm and placed the sample in a black trash bag with moist paper towels (to prevent the sample from drying out). The samples were stored at 4 °C in a refrigerator before hydraulic measurements. All samples were collected in the same day and hydraulic measurements were done within 3 days after sampling. For measurements of native hydraulic conductivity (K_h), a branch segment ~15 cm in length (~5 mm in diameter) was recut under water (to prevent further embolisms) from the middle part of the originally sampled branch 20-cm-long segment in the laboratory with the ends cleanly shaven with a fresh razor blade (Sperry et al. 1988, Liu et al. 2015). The samples were connected to the tubing system and perfused with a solution of 20 mM KCl. The perfusion solution was filtered to 0.22 μm pore diameter under 0.5 kpa pressure by vacuum pump (Vacuubrand MD1, GMBH, Germany) to remove air. A constant hydraulic head of 45 cm was used to generate a pressure that drove the solution flow through the segments and avoid flushing native embolism. Hydraulic conductivity (K_h, kg m s^{-1} MPa^{-1}) was calculated as:

$$K_h = \frac{J_V}{\Delta P/\Delta L} \quad (1)$$

where J_V is the flow rate through the branch segment (kg s^{-1}), and $\Delta P/\Delta L$ is the pressure gradient across the segment (MPa m^{-1}). Xylem-specific hydraulic conductivity (K_s, kg m^{-1} s^{-1} MPa^{-1}) was calculated as the ratio of K_h by the cross-sectional area of the xylem.

After measurement of K_h, the branch segments were submerged in perfusion solution (20 mM KCl) under a partial vacuum overnight (~24 h) to refill embolized vessels for the maximum hydraulic conductivity (K_{max}) measurements. The degree of xylem embolism was estimated by comparing K_h and K_{max} to calculate the native percentage loss of hydraulic conductivity (*PLC*). *PLC* was calculated as:

$$PLC = \frac{100\,(K_{max} - K_h)}{K_{max}} \quad (2)$$

Xylem anatomical traits

Xylem anatomical measurements were performed on cross-sections of the same current-year segments used for hydraulic

conductivity measurements. Paraffin sectioning and light microscopic observations methods were used. The procedure is described in Li (2009) and Spannl et al. (2016). Briefly, current-year branch segments ~0.5 cm were cut and fixed in FAA (70% formalin–acetic acid–alcohol, 43.5% ethanol 10% formalin 3% glacial acetic acid 43.5% 43.5% water) for at least 24 h. Each specimen was dehydrated with increasing ethanol concentration series (30%, 50%, 70%, 85%, 90% and ethanol) and cleared with xylene (TP1020, Leica, Germany), embedded in paraffin (HistoCore ArcadiaH+C, Leica, Germany) and cut into thin-sections (20 µm for branches and 12 µm for compound leaf petioles) with an electronic rotation microtome (RM2245,Leica, Germany). The sections were dewaxed with xylene and stained with safranin-fast green and the slides were examined under a light microscope (DM2500, Leica, Germany). Mean vessel diameter (*D*, µm) was estimated based on measurements of lumen area of all vessel appearing in the analyzed area of each image. Vessel density (*VD*, no.mm^{-2}) was determined as the number of vessels per xylem area. Image-J software (Image-J, 1.48u, USA) was used for data calculation.

Gas exchange

Gas exchange parameters including maximum net photosynthetic rate (A_{max}) and stomatal conductance (*gs*) were measured using a portable photosynthesis system (LI-6400XT, LI-COR Inc., USA). Measurements were made immediately after the long branches (~1.5 m) cut for hydraulic measurements. Sun-exposed portions and fully expanded leaves were selected for measuring and five data points were collected. For each measurement, chamber CO_2 concentration was set to 400 ppm (ambient) and sample chamber light was set to saturating light conditions of 1200 µmol m^{-2} s^{-1} (photosynthetically active radiation; PAR). We wished to avoid confounding light with species or treatment, hence this value was chosen both because it is above the light-saturation point for these species (Zhu et al. 2019), and it is typical of the above-canopy radiation these leaves were exposed to. A high flow rate (500 µmol s^{-1}) was set to minimize the time take for *A* and *gs* to stabilize and the leaf cuvette temperature was maintained at 26 ± 1.5 °C.

NSC analyses

Oven-dried leaf samples collected from the branches that were used for hydraulic traits measurements were ground to fine powder in a ball mill (MM400, Retsch, Germany). The concentrations of *NSC*, which are defined as soluble sugars and starch, were measured using the modified anthrone method (Hansen and Moller 1975, Mitchell et al. 2013). A total of 100 mg of leaf sample was weighed and extracted with 2 ml of 80% aqueous ethanol in a 10 ml polyethylene tube. The mixture was boiled in a water bath at 80 °C for 30 min, then centrifuged at 3500 rpm for 10 min. The supernatants were removed in a 25 ml volumetric flask and the procedure was repeated three times. The soluble sugar concentrations were determined using a predetermined standard curve by measuring the amount of glucose from UV–Vis spectrophotometer (Lambda 25, PerkinElmer, USA) of absorbance at 620 nm.

Starch was extracted from the residue with 2 ml distilled water and boiled in the water bath at 99.9 °C for 15 min, then added 2 ml 9.2 mol l^{-1} $HClO_4$, adding 4 ml distilled water after shaking the mixture for 15 min and centrifuged at 3500 rpm for 10 min. The supernatants were removed in a 50 ml volumetric flask and the procedure was repeated after replacing 9.2 mol l^{-1} $HClO_4$ with 4.6 mol l^{-1} $HClO_4$, then the residue was extracted with distilled water twice. Finally, starch concentration was determined by measuring glucose equivalents extracted from residue by $HClO_4$ according to a UV–Vis spectrophotometer of absorbance at 620 nm. We used glucose as the standard for both soluble sugar and starch concentration analyses.

C and N concentration, C/N ratio and leaf mass per area

Leaf samples were collected from each of the branches that were used for hydraulic traits measurements. Leaves were scanned for leaf area calculation using ImageJ software, then oven dried at 65 °C for at least 72 h until dry mass was constant within 0.01 g and milled with a ball mill. Leaf mass per area (LMA) was calculated as the leaf dry mass divided by the leaf area. Total C and N concentration were measured, and C/N ratio was analyzed with an elemental analyzer (Vario EL, Elementar, Germany).

Statistical analysis

Data were analyzed for normality and equal variance before the statistical analyses. The statistical significance of treatment effects was tested using one-way analysis of variance (ANOVA) and Tukey's HSD multiple comparisons were used to test the differences among treatments. Correlations between K_s and N addition treatment among the two species were fitted using Polynomial fit. The relationship between *PLC*, *NSC* and N addition rate were evaluated by linear regression analysis. Linear regressions were used to test for correlations between K_s, *PLC*, *NSC* and the xylem anatomical characteristics. Linear or polynomial fits were selected depending on the AIC. Results were considered statistically significant at $P < 0.05$. The SPSS 17 statistical package (SPSS Inc., Chicago, IL, USA) was used for statistical analysis.

Results

Response of hydraulic traits and xylem anatomy

The mean values of leaf water potential (Ψ_L) ranged from −0.88 MPa to −0.09 MPa and − 0.52 MPa to −0.23 MPa

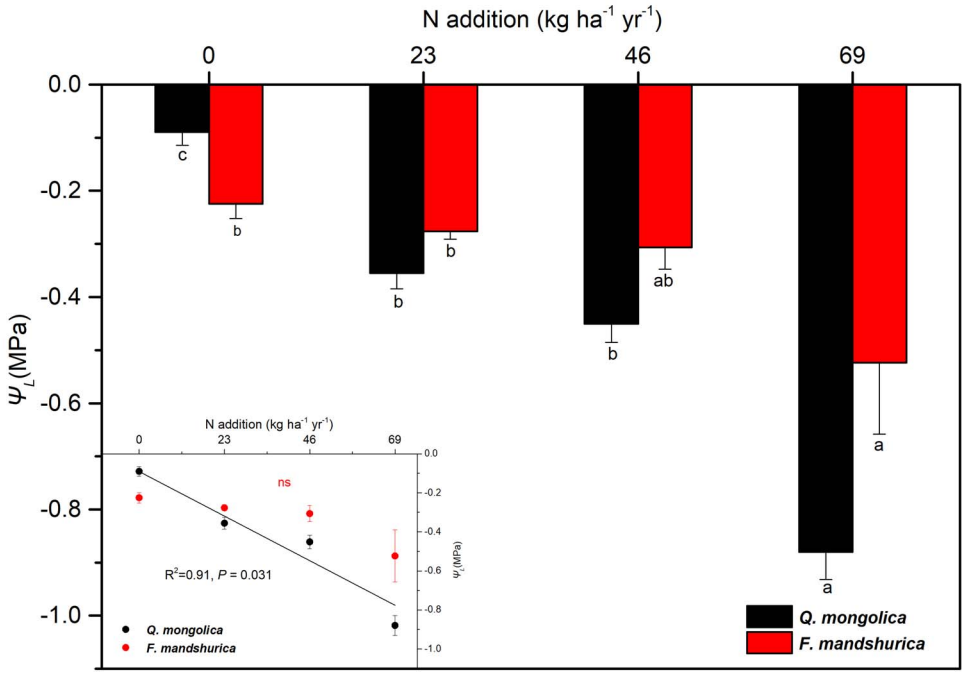

Figure 1. Responses of leaf water potential (Ψ_L, MPa) in *Q. mongolica* (black) and *F. mandshurica* (red) to different N addition treatments. The error bar represents ±1SE of all measurements for each individual tree species. Different letters indicate significant difference within each treatment for each species ($P < 0.05$). Linear regressions were fitted to the individual data in each species ($P < 0.05$).

in *Q. mongolica* and *F. mandshurica*, respectively. Ψ_L decreased with increasing N addition for both species (Figure 1), and this effect was significant in *Q. mongolica* ($P < 0.001$), but not in *F. mandshurica* ($P = 0.136$). Furthermore, the response pattern of water potential to different N addition treatments showed negative correlations (Figure 1). These effects were significant for *Q. mongolica* but not for *F. mandshurica*.

Overall, xylem-specific hydraulic conductivity (K_s) in both species significantly increased ($P = 0.032$ for *Q. mongolica*, $P = 0.010$ for *F. mandshurica*; ANOVA) after 7 years of N addition, but with a saturating response (see the polynomial fit analysis in Figure 2a). K_s of both species increased at low and medium N addition levels, but decreased with high N addition, with the highest K_s at an N addition level of 38.1 and 38.5 kg ha^{-1} yr^{-1} for *Q. mongolica* and *F. mandshurica*, respectively. Under different N addition levels, mean values of *PLC* measured varied from 4.19% to 34.39% in *Q. mongolica* and 9.04% to 29.40% in *F. mandshurica*. Percentage loss of hydraulic conductivity in both species significantly increased with N addition rate ($P = 0.001$ for *Q. mongolica*, $P = 0.009$ for *F. mandshurica*; ANOVA).

Consistent with the result of K_s, the vessel diameter first increased at low and medium N addition levels and then decreased at high N addition levels. Highest vessel diameter values were observed at medium levels of N fertilization among both species (Figure 4a). Vessel diameter significantly increased with N addition for both *Q. mongolica* ($P = 0.042$) and *F. mandshurica* ($P = 0.038$; Figure 4a; ANOVA). Vessel density of both species had a decreasing trend with N addition, which was significant for *F. mandshurica* ($P = 0.003$; Figure 4b). Notably, there were substantial differences in xylem anatomical traits between *F. mandshurica* and *Q. mongolica*, because *F. mandshurica* has compound leaf petioles, while *Q. mongolica* has no compound leaf petioles (Figure S1 available as Supplementary Data at *Tree Physiology* Online). We found that a semi-lignified architecture (the transitional growth stage to lignification) existed in compound leaf petiole (Figures 3 and S3). For compound leaf petioles, both vessel diameter and density had a significantly positive correlation with N addition according to linear or polynomial fit analysis (Figure 4). N addition increased both vessel diameter ($P = 0.046$, Figure 4a; ANOVA) and vessel density ($P = 0.047$, Figure 4b; ANOVA) of compound leaf petioles in *F. mandshurica*.

Responses of gas exchange and carbon reserves

A_{max} was strongly affected by N addition but *gs* was not, across the two species (Figure 5). A_{max} was significantly increased under N addition for both species, and the peak (highest) values were observed in medium N addition for *Q. mongolica* (Figure 5a). N addition did not change *gs* for the two species (except in high N addition for *Q. mongolica*; Figure 5b).

Overall, N addition has significantly increased soluble sugars for both *Q. mongolica* ($P = 0.005$) and *F. mandshurica* ($P = 0.009$), and has significantly decreased starch for both *Q. mongolica* ($P = 0.001$) and *F. mandshurica* ($P = 0.049$; ANOVA). Soluble sugars significantly increased under different

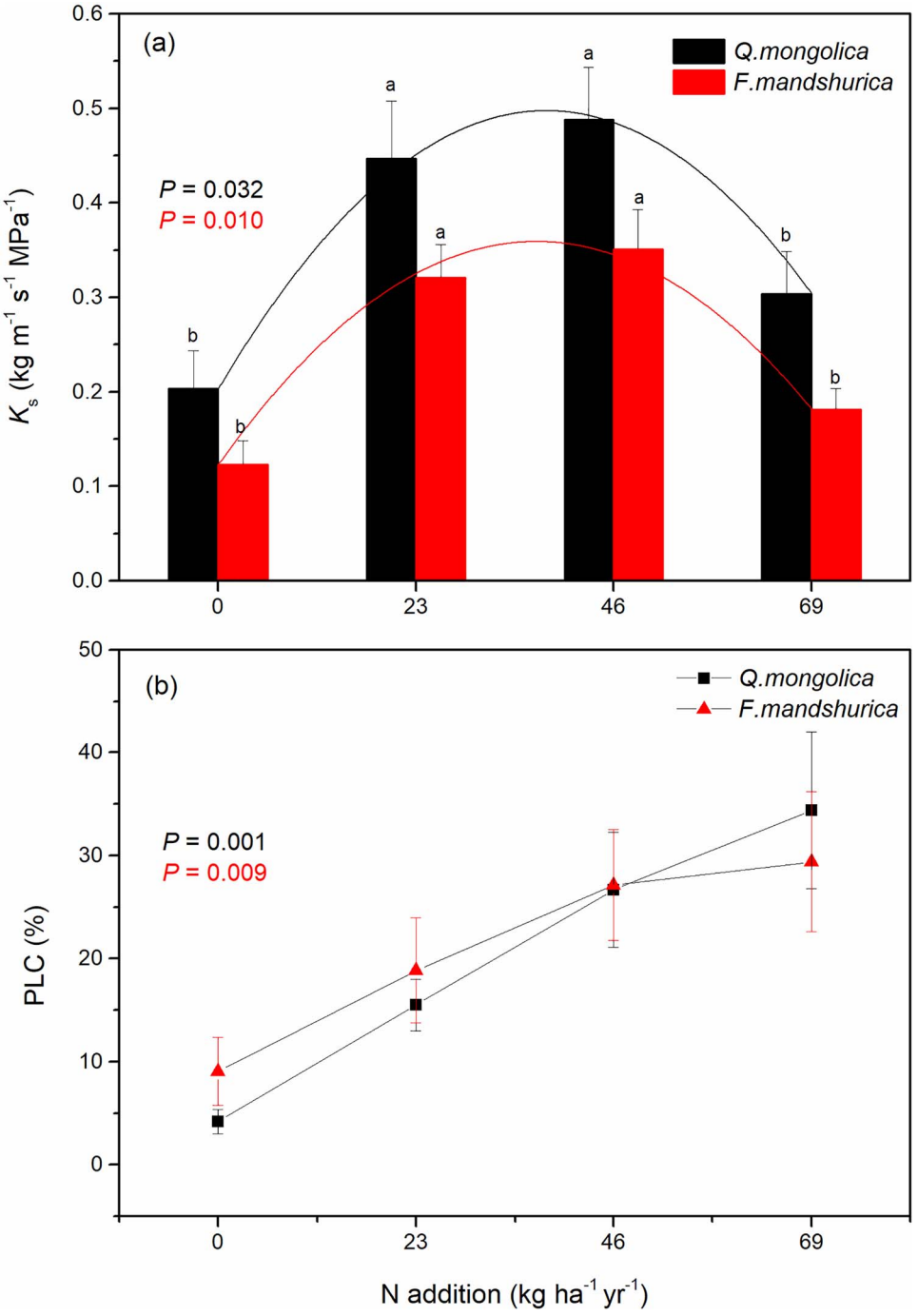

Figure 2. Responses of xylem-specific hydraulic conductivity (K_S) and the native percent loss of hydraulic conductivity (*PLC*) in *Q. mongolica* (black) and *F. mandshurica* (red) to different nitrogen (N) treatments (0, +23, +46, and + 69 kg N ha^{-1} year^{-1}). The error bar represents ±1SE. Different letters indicate significant difference within each treatment for each species ($P < 0.05$). Polynomial models were fitted to the individual data in each species of panel (a). The *P*-values were showed from ANOVA ($P < 0.05$).

N addition levels for both species except at low N addition level in *F. mandshurica* (Figure 6a). Starch significantly decreased under medium and high N addition levels for both *Q. mongolica* and *F. mandshurica* (Figure 6b). Nonstructural carbohydrate concentration was not significantly changed compared to control for both species, and medium and high N addition decreased NSC concentrations compared to low N addition for *Q. mongolica* (Figure 6c).

Values of foliar C concentration (C%) were not significantly changed for both species with N addition, while foliar N concentration (N%) was significantly increased (Table 1). N fertilization had significant effects on C/N ratio for both *Q. mongolica*

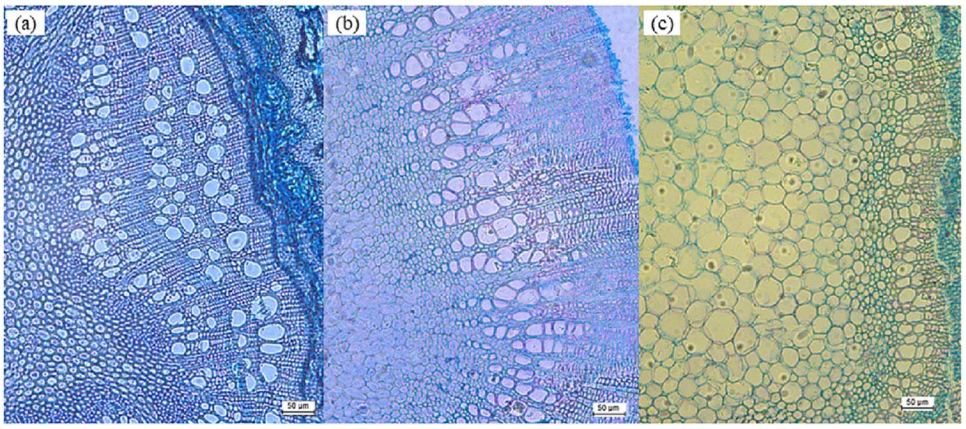

Figure 3. Light microscopy images of current-year branch cross-sections for *Q. mongolica* (a), *F. mandshurica* (b) and compound leaf petioles of *F. mandshurica* (c) in control. The images were taken under magnification of ×100.

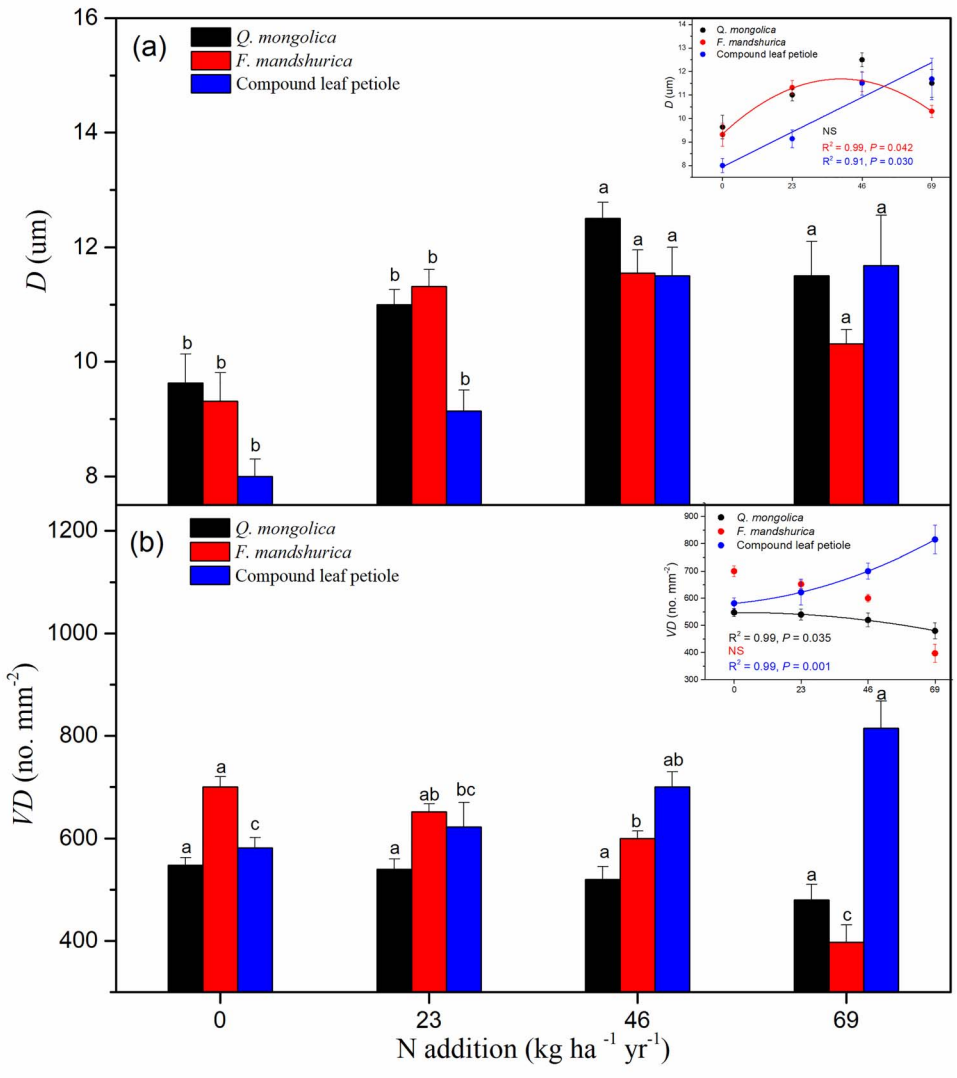

Figure 4. Responses of xylem mean vessel diameter and vessel density of current-year branches in *Q. mongolica* (black), *F. mandshurica* (red) and compound leaf petioles of *F. mandshurica* (blue) to different N addition levels. The error bar represents ±1SE of all measurements for each individual tree species. Different letters indicate significant difference within each treatment for each species ($P < 0.05$). Polynomial models or linear regressions were fitted to the individual data in each species ($P < 0.05$).

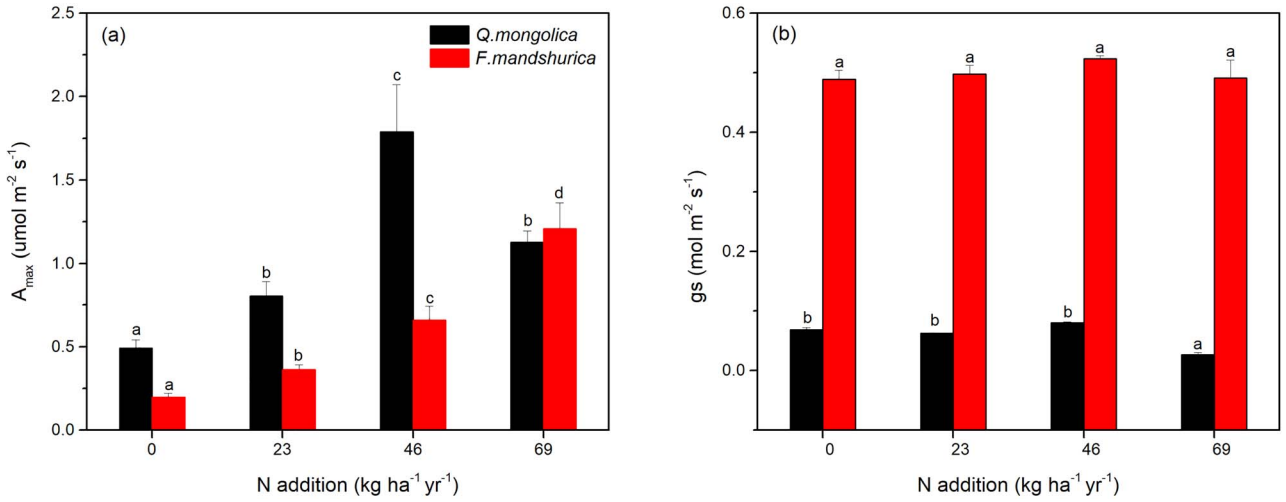

Figure 5. Responses of maximum net photosynthetic rate (A_{max}; a) and stomatal conductance (*gs*; b) responses in *Q. mongolica* and *F. mandshurica* to different N addition levels. The error bar represents 1SE of all measurements for each individual tree species. Different letters indicate significant difference within each treatment for each species ($P < 0.05$).

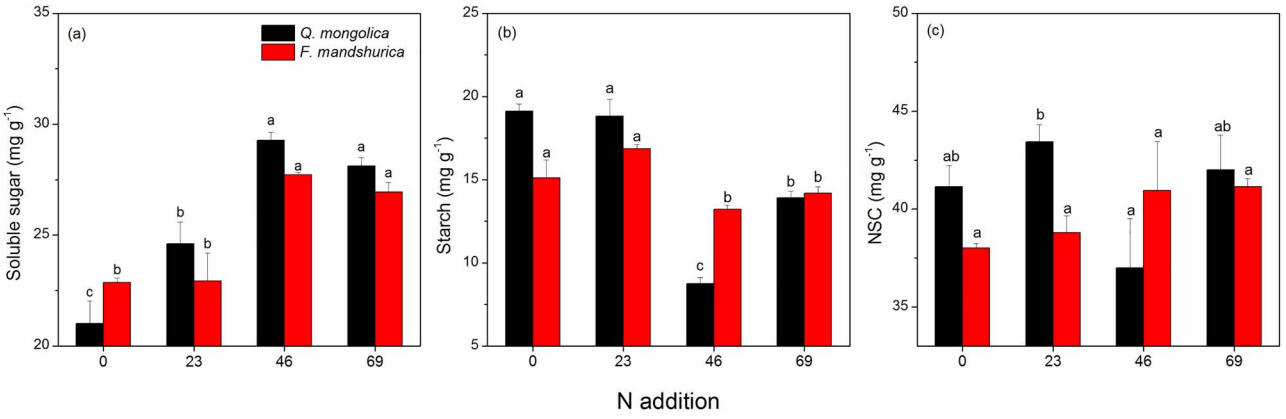

Figure 6. Responses of soluble sugar, starch concentration (mg g^{-1}) and total nonstructural carbohydrates (NSC) in *Q. mongolica* and *F. mandshurica* to different N addition levels. The error bar represents 1SE of all measurements for each individual tree species. Different letters indicate significant difference within each treatment for each species ($P < 0.05$).

Table 1. Functional traits relate to carbon dynamics measured under the control (0), low N addition (23 kg ha^{-1} yr^{-1}), medium N addition (46 kg ha^{-1} yr^{-1}) and high N addition (69 kg ha^{-1} yr^{-1}) treatments for *Q. mongolica* and *F. mandshurica*. Data are mean ± 1SE. Different letters indicate significant difference within each treatment for each species ($P < 0.05$). *P*-values are the results of one-way ANOVA and significance at $P < 0.05$ are presented in bold. C, foliar C concentration; N, foliar N concentration

Tree species	Variables	N addition (kg ha^{-1} yr^{-1})				*P*-value
		0	23	46	69	
Q. mongolica	C (%)	47.73 ± 0.33a	46.39 ± 0.16^{a}	47.53 ± 0.33^{a}	46.93 ± 0.10^{a}	0.062
	N (%)	2.80 ± 0.02^{a}	2.86 ± 0.04a	2.89 ± 0.03^{b}	3.21 ± 0.04^{c}	**0.003**
	C/N ratio	17.04 ± 0.61^{a}	16.39 ± 0.36^{a}	16.56 ± 0.66^{a}	14.62 ± 0.25^{b}	**0.046**
	LMA (g m^{-2})	56.28 ± 6.75^{a}	79.70 ± 2.28^{c}	72.78 ± 3.16^{b}	61.57 ± 1.17^{a}	**0.043**
F. mandshurica	C (%)	45.71 ± 0.35^{a}	45.32 ± 0.01^{a}	45.09 ± 0.62^{a}	46.56 ± 0.05^{a}	0.144
	N (%)	2.88 ± 0.24^{a}	3.15 ± 0.06^{a}	3.57 ± 0.04^{b}	3.71 ± 0.08^{b}	**0.032**
	C/N ratio	16.01 ± 0.44^{c}	14.41 ± 0.27^{b}	12.62 ± 0.05^{a}	12.59 ± 0.61^{a}	**0.010**
	LMA (g m^{-2})	44.48 ± 6.28^{a}	72.69 ± 1.85^{b}	53.46 ± 3.71^{a}	50.90 ± 1.45^{a}	**0.025**

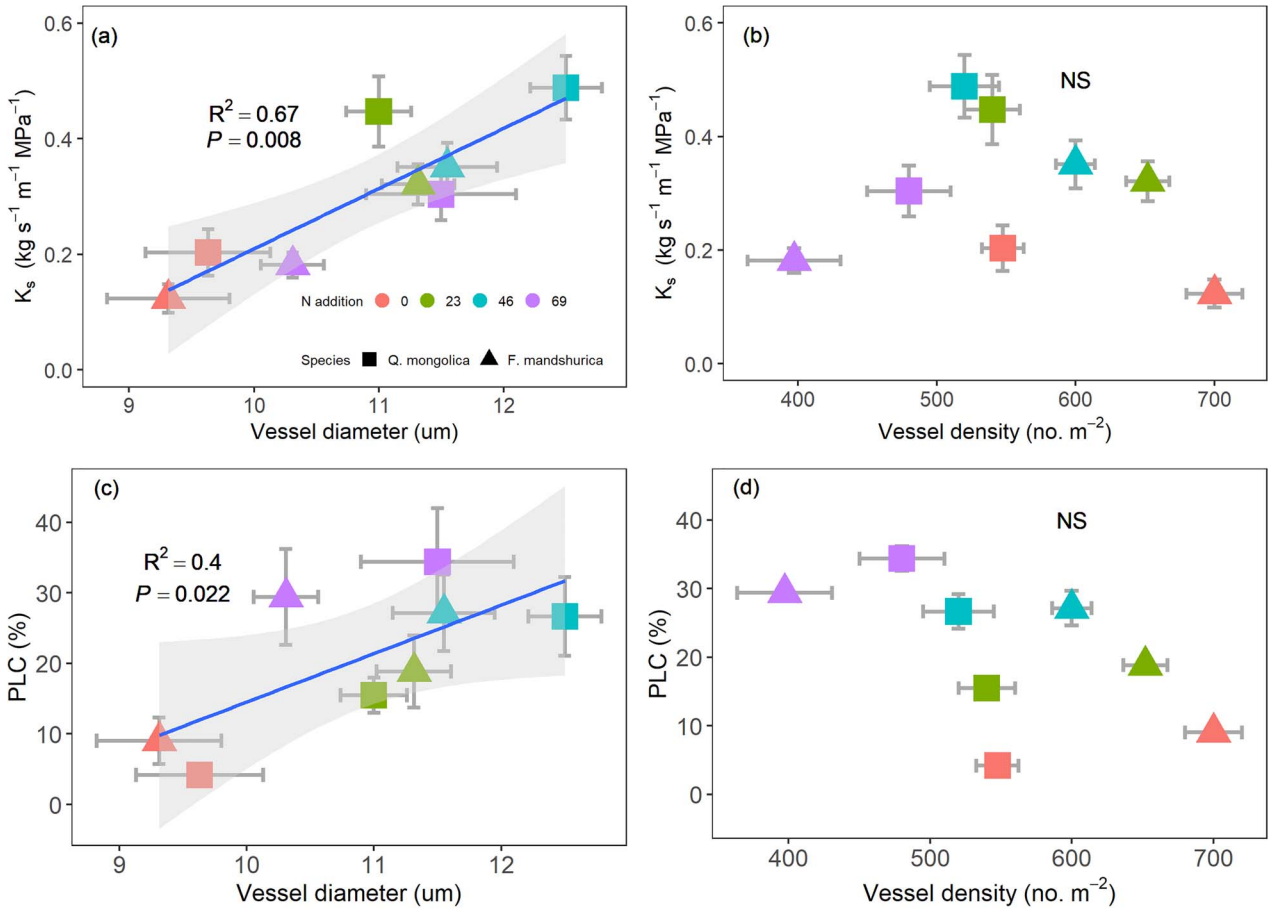

Figure 7. The relationship between xylem-specific hydraulic conductivity (K_s), the percent loss of hydraulic conductivity (*PLC*, %) and vessel diameter and vessel density across the two species. The error bar represents ±1SE of all measurements for each individual tree species. Linear regressions were fitted to the individual data ($P < 0.05$).

and *F. mandshurica* (Table 1). The effects of N addition on LMA were significant in both *Q. mongolica* and *F. mandshurica*. Furthermore, *LMA* significantly increased at low and medium N addition levels compared to control for *Q. mongolica*, but significantly increased only at low N addition level for *F. mandshurica* (Table 1).

The relationships among hydraulics, gas exchange and carbon reserves under N addition

K_s had significant positive correlations with vessel diameter among the two species but K_s did not correlate with vessel density (Figure 7a and b). This pattern was similar for *PLC* (Figure 7c and d). In addition, A_{max} had a significant positive correlation with vessel diameter but not with vessel density (Figure 8a and b). Consistently, vessel diameter positively correlated with soluble sugar concentration but not with vessel density (Figure 8c and d). We also found K_s had a significant positive correlation with *LMA* (Figure S4 available as Supplementary Data at *Tree Physiology* Online).

A_{max} was positively related to foliar N concentration (Figure 9a), soluble sugars was positively related to A_{max} (Figure 9b) and *PLC* has significant positive correlation with soluble sugars (Figure 9c), but no significant correlation was observed between K_s and *PLC* (Figure 9d). Note that both species had low efficiency and high hydraulic safety under normal growth condition (Figure 9d).

The results of principal component analysis (PCA) showed that PC axes 1 explained 42.5% of the total variation and was strongly related to carbohydrates reserves (i.e., soluble sugars, starch), A_{max}, PLC, hydraulic architecture (i.e., vessel diameter, vessel density) and leaf water potential (Figure 10). PC axes 2 explained 26.2% of the total variation and was related to *gs*, K_s, foliar C and N concentration, C/N ratio and *LMA*. The species were clearly arranged by different N addition levels in the space defined by the two PC axes (Figure 10b). Analysis of *Q. mongolica* under different N addition treatments clustered at the positive side of PC axes 2, whereas *F. mandshurica* were loaded at the negative side of PC axes 2.

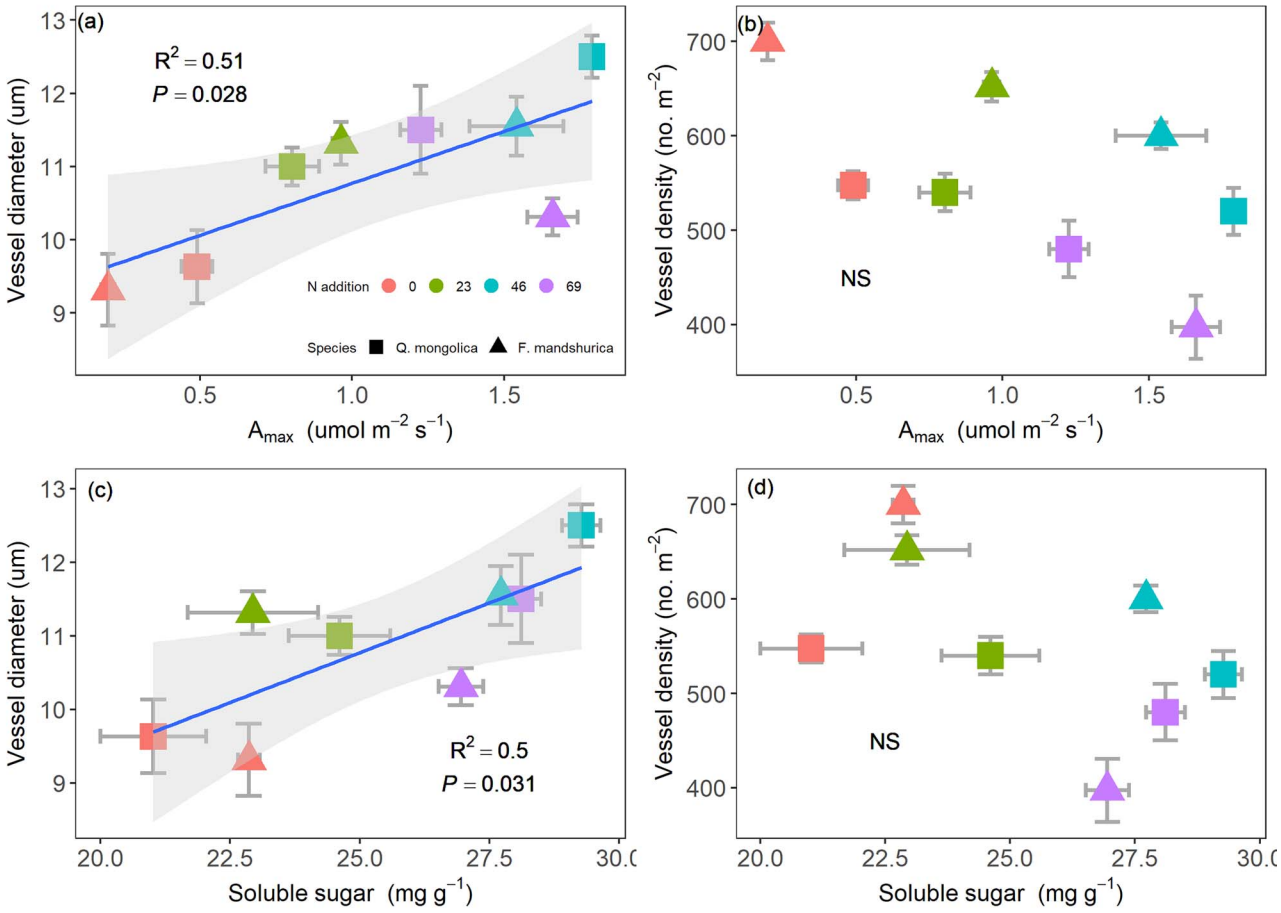

Figure 8. The relationship between vessel diameter and vessel density, and maximum net photosynthetic rate (A_{max}) and soluble sugars across the two species. The error bar represents ±1SE of all measurements for each individual tree species. Linear regressions were fitted to the individual data ($P < 0.05$).

Discussion

We investigated the shifts of tree functional traits under seven-year N addition based on water relations (hydraulics), carbon source (gas exchange) and carbon reserve (*NSC*) levels. This approach allowed an assessment of coordination of hydraulics, gas exchange and carbon reserves under N deposition. Consistent with our first hypothesis, we found that N addition significantly increased vessel diameter and thus enhanced xylem-specific hydraulic conductivity (K_s). However, wider vessel diameters under N addition could also lead to a higher risk of xylem embolism from freezing (Pittermann and Sperry 2003, Hacke et al. 2006), which is consistent with the increased *PLC* we observed with higher N addition. In addition, the results support our second hypothesis that N addition increased maximum net photosynthetic rate in association with increased foliar N concentration while *gs* remained unchanged. Furthermore, N addition significantly reduced starch concentration but increased soluble sugar concentration across the two species we examined. Our results are consistent with the idea that soluble sugars play a critical role in restoring hydraulic function in trees that experience annual freeze–thaw embolism under high N availability as indicated by the positive correlations between soluble sugars and both vessel diameter and *PLC*.

Hydraulic shifts with long-term N addition

Both tree species showed significant increases in hydraulic conductivity under N addition (Figure 2), and the enhanced hydraulic efficiency was mainly attributed to increased conduit dimensions (e.g., wider vessel diameter; Figure 8a), although conduit length was not observed in our study. This is inconsistent with the results by Wang et al. (2016), who demonstrated that N addition significantly increased vessel diameter but did not lead to any positive effects on hydraulic conductance in *F. mandshurica* seedlings. This discrepancy is presumably resulted by the difference between seedlings and field mature trees (Hartmann et al. 2018). The faster growth rate in seedlings under optimal N fertilization seems to have a cost in terms of reduced whole-plant hydraulic conductance (Phillips et al. 2001, Goldstein et al. 2013), but for mature trees with

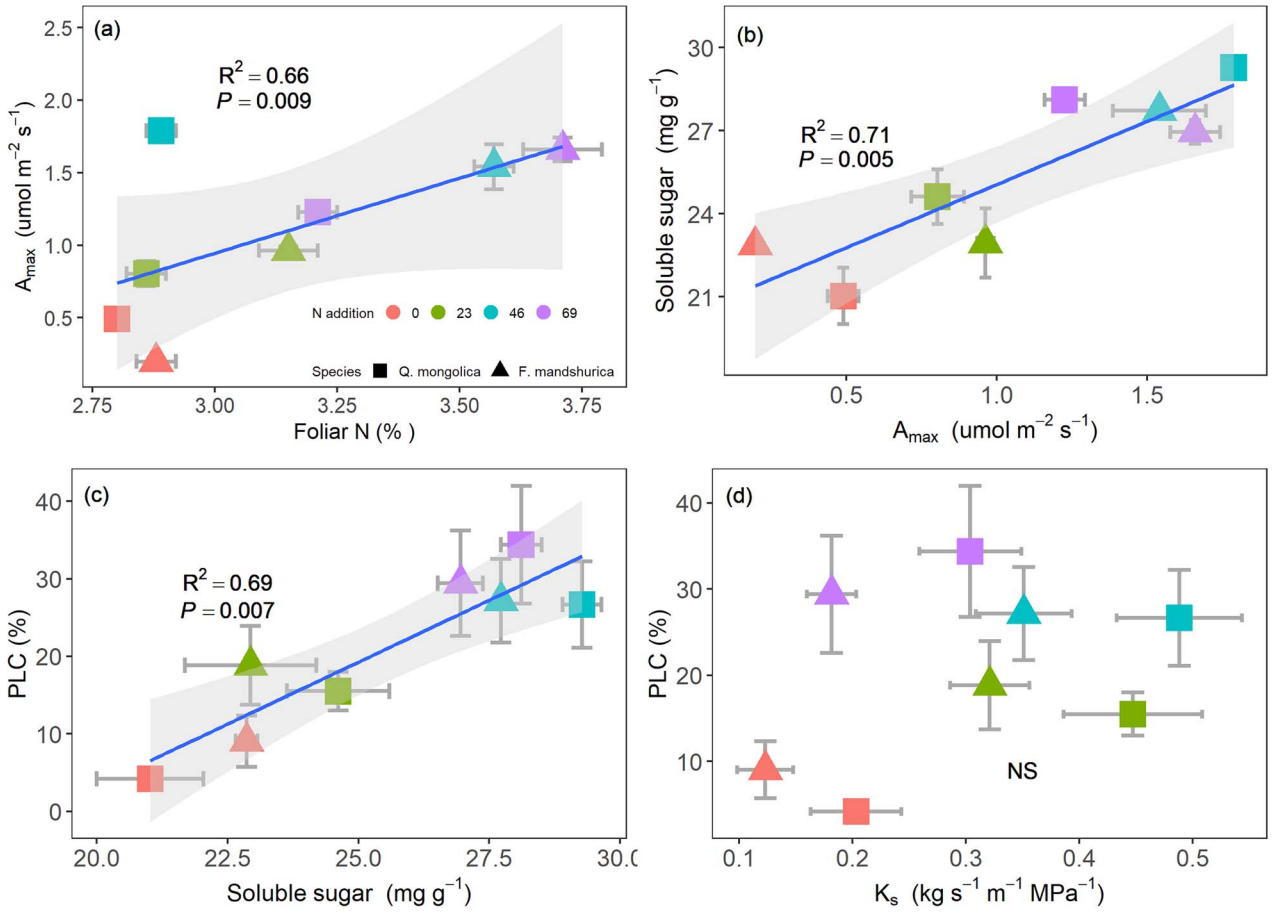

Figure 9. The relationship between maximum net photosynthetic rate (A_{max}) and foliar N concentration (a); between soluble sugars and *A* (b); between the percent loss of hydraulic conductivity (*PLC*) and soluble sugars (c); and between *PLC* and hydraulic conductivity (K_s) across the two species. The error bar represents ±1SE of all measurements for each individual tree species. Linear regressions were fitted to the individual data ($P < 0.05$).

established root systems N fertilization may exert more benefits for water transport (Bucci et al. 2006).

For the two species we examined, wider vessel diameters under N-addition (Figure 4) are more likely to allow gas bubbles to form (cavitation leading to emboli) in conduits during the sap freezing process and thus species with relatively large xylem conduits are found to be more vulnerable to freeze–thaw stress, this freeze–thaw-induced xylem embolism generally occurred in temperate tree species, which may decrease hydraulic safety (Davis et al. 1999, Hacke et al. 2006, Niu et al. 2017). This is consistent with our results that N addition significantly increased *PLC* and decreased leaf water potential (more negative) in this study (Figures 1, 2 and 4). Our previous study also found that N addition decreased leaf water potential but increased P50 (P50, water potential corresponding to 50% loss of hydraulic conductivity; Zhang et al. 2018). This may be related to the accumulation of soluble sugars or increased risk of embolism. A gradual increase in *PLC* with declining water potential under N addition could represent cavitation of the larger vessels. This inference is consistent with a previous study that reported an increase in both xylem efficiency and cavitation with high nutrient availability in trees (Goldstein et al. 2013). However, further work would be needed to quantify shifts in vulnerability.

The highest hydraulic conductivity and vessel diameter occurred at moderate levels of N addition for the two species, and thereafter decreased with further increases of N addition (Figures 2 and 4), suggesting that water transport efficiency increased with soil N availability to a threshold (about 38 kg ha^{-1} yr^{-1}; see results section). Based on our results, we can infer that there should be N-limited in the system, and that when the N addition levels exceed the threshold, the N effects will disappear. The negative effects of excessive N addition are likely attributed to one of the following reasons: greater risk of xylem cavitation; nutrient imbalances and a decrease in leaf mass per unit area with excessive N addition (*LMA*; Table 1, Figure S4 available as Supplementary Data at *Tree Physiology* Online). Sustained and continuous N supplies increased foliar N content (thereby declining foliar C/N ratio; Table 1), which could aggravate other nutrient limitations (e.g.,

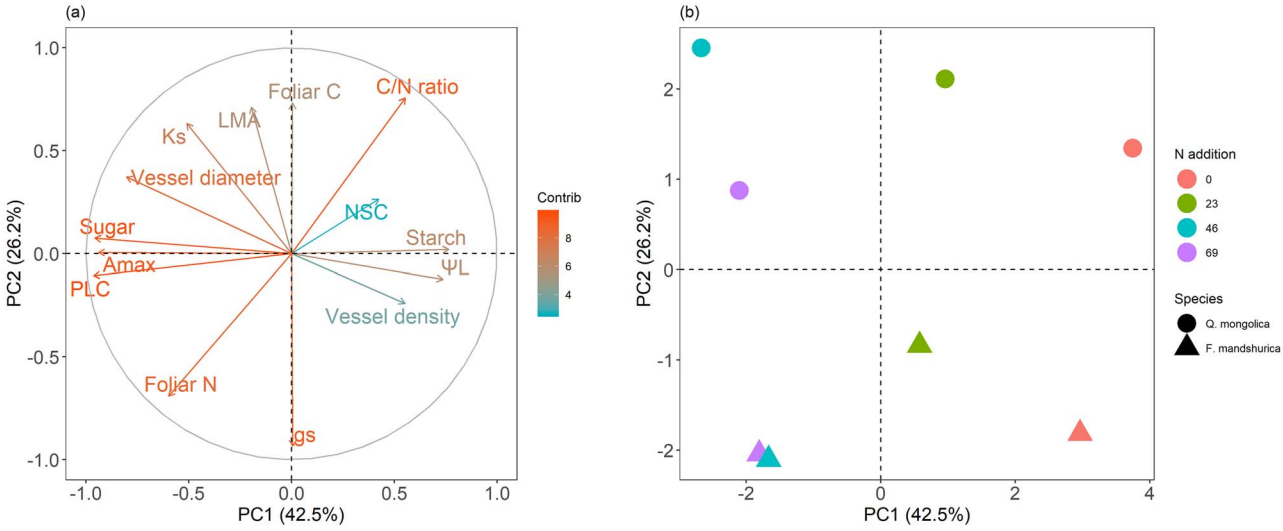

Figure 10. Principal component analysis of two tree species with different N addition levels based on 14 functional traits we measured. The percentages in the axis labels indicate the variance explained by the axis. PC axes 1 and PC axes 2 explain 42.5% and 26.2% of the total variation, respectively. (a) Analysis of 14 functional traits. Ψ_L, leaf water potential; K_s, xylem-specific hydraulic conductivity; *PLC*, native percent loss of conductivity; A_{max}, maximum net photosynthetic rate; *gs*, stomatal conductance; *LMA*, leaf mass per area; *NSC*, nonstructural carbohydrates; foliar C, foliar C concentration; foliar N, foliar N concentration; C/N ratio, foliar C/N ratio; sugar, soluble sugars; (b) Analysis of two woody species under different N addition treatments.

potassium, phosphorus; Huang et al. 2016, Liu et al. 2016, Xiao et al. 2017). These mixed-proportional responses were part of a web of scaling relationships mediated by plasticity in *LMA* (Figures 5 and S4).

Our results suggest that N-induced changes in xylem architecture and hydraulic efficiency varied across two species we examined. Increased vessel diameter and xylem hydraulic conductivity with N addition in *Q. mongolica* (simple-leaved species) were apparently greater compared to *F. mandshurica* (compound-leaved species; Figure 4a), which could result in a relatively rapid increase of *PLC* and decline of water potential in *Q. mongolica* under high N addition. The different hydraulic strategies among the two species might relate to the difference isolation of vessels, highly connected networks in *F. mandshurica* may propagate emboli more readily than *Q. mongolica* with more isolated vessels. This is consistent with our previous results conducted with same seedling species at same site (Zhang et al. 2019). We also found that N addition significantly decreased vessel density in *F. mandshurica*, but not in *Q. mongolica* (Figure 4b). Notably, the compound leaf petioles in *F. mandshurica* are a semi-lignified architecture, and both vessel diameter and vessel density of compound leaf petioles were significantly increased (Figures 3 and 4). Hence, we can speculate that N addition promoted xylem structure growth, including the transformation of xylem from semi-lignified to lignified in compound leaf petioles of *F. mandshurica* (Figure S3 available as Supplementary Data at *Tree Physiology* Online), which might benefit for water transport. However, the details of transformation of semi-lignified hydraulic architecture are not well-resolved in our data, nor yet in the literature. The differences in hydraulic architecture among species result in different hydraulic system, which might be the key functional attribute determining the species-specific responses to environmental changes (Tyree and Ewers 1991, Patino et al. 1995, Beikircher and Mayr 2008, Nicotra et al. 2010, Zhang et al. 2019).

Divergences in gas exchange for N addition across the tree species

N addition significantly increased foliar N concentration and maximum net photosynthetic rate (Figure 5, Table 1),and the increased maximum net photosynthetic rate was positively correlated with foliar N concentration (Figure 9a), which is consistent with previous results that leaf N concentrations play critical roles in photosynthetic capacity (Field et al. 1989, Quinn Thomas et al. 2009, Sparks 2009, Schulte-Uebbing and de Vries 2018). Enhanced photosynthesis with N addition could stimulate carbohydrate supply (Li et al. 2020), which is consistent with our result that N addition significantly increased soluble sugar concentration in foliage (Figures 5 and 6). In addition, we found that N addition did not alter *gs* across the two species but *F. mandshurica* showed much higher *gs* than *Q. mongolica* (Figure 5), suggesting that *F. mandshurica* had a stronger gas exchange capacity. These differences between the two tree species may be because compound-leaved tree species are more likely to protect themselves from unfavorable environmental conditions via stomatal control (Gorai et al. 2015). In addition, compound leaf petioles showed a higher hydraulic safety compared to the leaflet laminas in compound-leaved species (Liu et al. 2015), and compound-leaved species

have higher hydraulic conductance at the whole-branch level than simple-leaved species (Yang et al. 2018). This allows compound-leaved species to minimize the risk of catastrophic embolism in stems by sacrificing the whole compound leaves, which requires high gas exchange rate to compensate for their extra carbon losses (Niinemets 1998, Yang et al. 2018, Zhang et al. 2019).

Potential influence of NSC on the coupled responses of tree functional traits to N addition

N addition increased simple sugar production through photosynthesis and starch hydrolysis (starch decreased; Figure 6), thereby increasing soluble sugar concentration in foliage (Figure 6), which are likely important in maintaining the osmotic potentials necessary for seasonal recovery. We speculate that increased soluble sugars could be used for regulating hydraulic function as indicated by positive correlations between soluble sugar concentrations and hydraulic traits (*PLC* and vessel diameter; Figures 8 and 9) in our study. This is consistent with previous results that NSC storage and its remobilization are coupled with tree hydraulic functionality under high embolism risks (Chapin et al. 1990, Holbrook et al. 1999, Secchi and Zwieniecki 2012, Galvez et al. 2013, Dietze et al. 2014, Wang et al. 2018). Our previous studies also found that N addition can change carbon partitioning patterns via increasing photosynthetic rate and intrinsic water-use efficiency (*i*WUE) and thus might affect hydraulic shifts (Zhang et al. 2018, Li et al. 2020). However, sugar content measurement in our study was limited in leaves, future experiments that quantify sugars in other organs (for example, in stems/shoots) were required. In addition, our PCA results showed that high photosynthesis, soluble sugar concentration and native *PLC* co-occurred under N addition in the two tree species (at the negative side of PC axes and close to PC axes 2; Figure 10a), suggesting a strong trade-off among these three functional traits. Hence, these large changes in tree hydraulic systems and carbon functional attributes indicate that N nutrient availability has significant coupled effects on both water and carbon economy of woody plants (Salifu & Timmer 2001, Salleo et al. 2009, Martin et al. 2010), suggesting that *NSC* might mitigate the trade-offs between xylem safety and xylem-specific hydraulic efficiency, reflected in the absence of correlation between K_s and *PLC* in our results (Figure 9).

Concluding remarks

In this study, we investigated the water transport capacity associated with xylem anatomy, gas exchange and carbon reserves across two tree species under seven-year nitrogen addition. N addition increased vessel diameter thereby promoting hydraulic efficiency and decreased hydraulic safety. Divergent plant structure among species might lead to different hydraulic strategies to stress tolerance. Furthermore, hydraulic conductivity reached maximum rates at the medium N addition levels, suggesting that excessive N addition showed negative effects on hydraulic efficiency. Most notably, increased soluble sugar concentration under N addition was associated with changes of photosynthetic rate, percentage loss of hydraulic conductivity and vessel diameter, suggesting that carbohydrates might mitigate the trade-offs between hydraulic efficiency and safety under N addition. The linkage between hydraulic traits and nonstructural carbohydrates shown in this study leads us consider the ecological implication of coupled strategies for forest ecosystems under increasing atmospheric N deposition. This description of coordination of functional traits could provide a complete view of tree adaptation to the environment.

Supplementary Data

Supplementary Data for this article are available at *Tree Physiology* Online.

Acknowledgments

We greatly appreciate the support and technical assistance from the Eco-climatology research group. We are grateful for the staff of the Research Station of Changbai Mountain Forest Ecosystems of Chinese Academy of Sciences for their help in laboratory. We would like to thank Hao Xu for their assistance in the field. We also would like to thank Elizabeth Weiss for language editing.

Conflict of interest

None declared.

Funding

This work was supported by the National Natural Science Foundation of China (Grant Nos. 41675112, 31670707, 31870625, 31400541) and Pacific Northwest National Laboratories LDRD program.

Authors' contributions

H.X.Z, D.X.G and F.H.Y designed the study; H.X.Z, A.Z.W, W.B.L, C.J.J and J.Y.T collected the data; H.X.Z wrote the first draft of the manuscript, and N.G.M and A.L.P. provided valuable edits to the manuscript. All authors contributed to the data analysis and revisions.

References

Adams HD, Zeppel MJ, Anderegg WR et al. (2017) A multi-species synthesis of physiological mechanisms in drought-induced tree mortality. Nat Ecol Evol 1:1285–1291.

Anderegg WRL, Anderegg LDL (2013) Hydraulic and carbohydrate changes in experimental drought-induced mortality of saplings in two conifer species. Tree Physiol 33:252–260.

Beikircher B, Mayr S (2008) The hydraulic architecture of Juniperus communis L. ssp communis: shrubs and trees compared. Plant Cell Environ 31:1545–1556.

Borghetti M, Gentilesca T, Leonardi S, van Noije T, Rita A (2017) Long-term temporal relationships between environmental conditions and xylem functional traits: a meta-analysis across a range of woody species along climatic and nitrogen deposition gradients. Tree Physiol 37:4–17.

Bucci SJ, Scholz FG, Goldstein G et al. (2006) Nutrient availability constrains the hydraulic architecture and water relations of savannah trees. Plant Cell Environ 29:2153–2167.

Chapin FSI, Schulze E, Mooney HA (1990) The ecology and economics of storage in plants. Annu Rev Ecol Evol Syst 21:423–447.

Clifford S, Arndt S, Corlett J, Joshi S, Sankhla N, Popp M, Jones H (1998) The role of solute accumulation, osmotic adjustment and changes in cell wall elasticity in drought tolerance in Ziziphus mauritiana (Lamk.). J Exp Bot 49:967–977.

Davidson EA (2009) The contribution of manure and fertilizer nitrogen to atmospheric nitrous oxide since 1860. Nat Geosci 2: 659–662.

Davis SD, Sperry JS, Hacke UG (1999) The relationship between xylem conduit diameter and cavitation caused by freezing. Am J Bot 86:1367–1372.

Dichio B, Margiotta G, Xiloyannis C, Bufo S, Sofo A, Cataldi T (2009) Changes in water status and osmolyte contents in leaves and roots of olive plants (*Olea europaea L.*) subjected to water deficit. Trees 23: 247–256.

Dietze MC, Sala A, Carbone MS, Czimczik CI, Mantooth JA, Richardson AD, Vargas R (2014) Nonstructural carbon in woody plants. Annu Rev Plant Biol 65:667–687.

Evans JR (1989) Photosynthesis and nitrogen relationships in leaves of C3 plants. Oecologia 78:9–19.

Fang LD, Zhao Q, Liu YY, Hao GY (2017) The influence of a five-year nitrogen fertilization treatment on hydraulic architecture of Pinus sylvestris var. mongolica in a water-limited plantation of NE China. For Ecol Manage 418:15–22.

Fatichi S, Leuzinger S, Körner C (2014) Moving beyond photosyn thesis from carbon source to sink vegetation modeling. New Phytol 201:1086–1095.

Field CH. and Mooney HA (1986) Photosynthesis–nitrogen relationship in wild plants. In On the Economy of Plant Form and Function. Proceedings of the Sixth Maria Moors Cabot Symposium, Evolutionary Constraints on Primary Productivity, Adaptive Patterns of Energy Capture in Plants, Harvard Forest, August 1983. Cambridge [Cambridgeshire]: Cambridge University Press, c1986.

Fonti P, von Arx G, García-González I, Eilmann B, Sass-Klaassen U, Gärtner H, Eckstein D (2010) Studying global change through investigation of the plastic responses of xylem anatomy in tree rings. New Phytol 185:42–53.

Fowler D, Coyle M, Skiba U et al. (2013) The global nitrogen cycle in the twenty-first century. Philos Trans R Soc Lond B Biol Sci 368: 20130164.

Galiano L, Martinez Vilalta J, Lloret F (2011) Carbon reserves and canopy defoliation determine the recovery of scots pine 4 yr after a drought episode. New Phytol 190:750–759.

Galloway JN, Townsend AR, Erisman JW et al. (2008) Transformation of the nitrogen cycle: recent trends, questions, and potential solutions. Science 320:889–892.

Galvez D, Landhäusser S, Tyree M (2013) Low root reserve accumulation during drought may lead to winter mortality in poplar seedlings. New Phytol 198:139–148.

Goldstein G, Bucci SJ, Scholz FG (2013) Why do trees adjust water relations and hydraulic architecture in response to nutrient availability? Tree Physiol 33:238–240.

Gorai M, Laajili W, Santiago L, Neffati M (2015) Rapid recovery of photosynthesis and water relations following soil drying and re-watering is related to the adaptation of desert shrub Ephedra alata subsp. alenda (Ephedraceae) to arid environments. Environ Exp Bot 109:113–121.

Grassi G, Meir P, Cromer R, Tompkins D, Jarvis PG (2002) Photosynthetic parameters in seedlings of Eucalyptus grandis as affected by rate of nitrogen supply. Plant Cell Environ 25:1677–1688.

Hacke U, Sperry J (2003) Limits to xylem refilling under negative pressure in Laurus nobilis and Acer negundo. Plant Cell Environ 26:303–311.

Hacke UG, Plavcová L, Almeida-Rodriguez A, King-Jones S, Zhou W, Cooke JEK (2010) Influence of nitrogen fertilization on xylem traits and aquaporin expression in stems of hybrid poplar. Tree Physiol 30:1016–1025.

Hacke UG, Sperry JS, Wheeler JK, Castro L (2006) Scaling of angiosperm xylem structure with safety and efficiency. Tree Physiol 26:689–701.

Hansen J, Moller I (1975) Percolation of starch and soluble carbohydrates from plant-tissue for quantitative-determination with anthrone. Anal Biochem 68:87–94.

Hartmann H, Adams HD, Hammond WM, Hoch G, Landhäusser SM, Wiley E, Zaehle S (2018) Identifying differences in carbohydrate dynamics of seedlings and mature trees to improve carbon allocation in models for trees and forests. Environ Exp Bot 152:7–18.

Hartmann H, Trumbore S (2016) Understanding the roles of non-structural carbohydrates in forest trees–from what we can measure to what we want to know. New Phytol 211:386–403.

Harvey HP, Van den Driessche R (1999) Nitrogen and potassium effects on xylem cavitation and water-use efficiency in poplars. Tree Physiol 19:943–950.

Hoegberg P, Fan H, Quist M, Binkley D, Tamm CO (2006) Tree growth and soil acidification in response to 30 years of experimental nitrogen loading on boreal forest. Glob Chang Biol 12:489–499.

Holbrook N, Zwieniecki MA (1999) Embolism Repair and Xylem Tension: Do We Need a Miracle? Plant physiol 120:7–10.

Huang ZQ, Liu B, Davis M, Sardans J, Penuelas J, Billings S (2016) Long-term nitrogen deposition linked to reduced water use efficiency in forests with low phosphorus availability. New Phytol 210:431–442.

Keenan TF, Hollinger DY, Bohrer G, Dragoni D, Munger JW, Schmid HP, Richardson AD (2013) Increase in forest water-use efficiency as atmospheric carbon dioxide concentrations rise. Nature 499:324.

Leonardi S, Gentilesca T, Guerrieri R et al. (2012) Assessing the effects of nitrogen deposition and climate on carbon isotope discrimination and intrinsic water-use efficiency of angiosperm and conifer trees under rising CO2 conditions. Glob Chang Biol 18:2925–2944.

Li HP (2009) Plant microscopy techniques. In: Chapter (iii), examples of paraffin sectioning. Science Press, Beijing, pp 285–287.

Li W, Bai Z, Jin C et al. (2017) The influence of tree species on small scale spatial heterogeneity of soil respiration in a temperate mixed forest. Sci Total Environ 590-591:242–248.

Li W, Hartmann H, Adams HD et al. (2018) The sweet side of global change-dynamic responses of non-structural carbohydrates to drought, elevated CO2 and nitrogen fertilization in tree species. Tree Physiol 38:1706–1723.

Li W, Jin C, Guan D, Wang Q, Wang A, Yuan F, Wu J (2015) The effects of simulated nitrogen deposition on plant root traits: a meta-analysis. Soil Biol Biochem 82:112–118.

Li W, Zhang H, Huang G, Liu R, Wu H, Zhao C, McDowell NG (2020) Effects of nitrogen enrichment on tree carbon allocation: a global synthesis. Glob Ecol Biogeogr 29:573–589.

Liu J, Wu N, Wang H, Sun J, Peng B, Jiang P, Bai E (2016) Nitrogen addition affects chemical compositions of plant tissues, litter and soil organic matter. Ecology 97:1796–1806.

Liu YY, Song J, Wang M, Li N, Niu CY, Hao GY (2015) Coordination of xylem hydraulics and stomatal regulation in keeping the integrity of xylem water transport in shoots of two compound-leaved tree species. Tree Physiol 35:1333–1342.

IPCC (2007) Climate Change 2007: The Physical Science Basis. Cambridge: Cambridge University Press.

Lovelock CE, Feller IC, Mckee KL, Engelbrecht BMJ, Ball MC (2004) The effect of nutrient enrichment on growth, photosynthesis and hydraulic conductance of dwarf mangroves in Panamá. Func Ecol 18:25–33.

Magill AH, Aber JD, Currie WS et al. (2004) Ecosystem response to 15 years of chronic nitrogen additions at the Harvard forests LTER, Massachusetts, USA. For Ecol Manage 196:7–28.

Magnani F, Grace J, Borghetti M (2002) Adjustment of tree structure in response to the environment under hydraulic constraints. Func Ecol 16:385–393.

Martin KC, Bruhn D, Lovelock CE, Feller IC, Evans JR, Ball MC (2010) Nitrogen fertilization enhances water-use efficiency in a saline environment. Plant Cell Environ 33:344–357.

Mcdowell NG (2011) Mechanisms linking drought, hydraulics, carbon metabolism, and vegetation mortality. Plant Physiol 155:1051–1059.

Mitchell PJ, O'Grady AP, Tissue DT, White DA, Ottenschlaeger ML, Pinkard EA (2013) Drought response strategies define the relative contributions of hydraulic dysfunction and carbohydrate depletion during tree mortality. New Phytol 197:862–872.

Mitchell PJ, O'Grady AP, Tissue DT, Worledge D, Pinkard EA (2014) Co-ordination of growth, gas exchange and hydraulics define the carbon safety margin in tree species with contrasting drought strategies. Tree Physiol 34:443–458.

Mozdzer TJ, Caplan JS (2018) Complementary responses of morphology and physiology enhance the stand-scale production of a model invasive species under elevated CO2 and nitrogen. Func Ecolo 32:1784–1796.

Nardini A, Lo Gullo MA, Salleo S (2011) Refilling embolized xylem conduits: is it a matter of phloem unloading? Plant Sci 180:604–611.

Nicotra AB, Atkin OK, Bonser SP et al. (2010) Plant phenotypic plasticity in a changing climate. Trends Plant Sci 15:684–692.

Niinemets Ü (1998) Are compound-leaved woody species inherently shade-intolerant? An analysis of species ecological requirements and foliar support costs. Plant Ecol 134:1–11.

Niu CY, Meinzer FC, Hao GY (2017) Divergence in strategies for coping with winter embolism among co-occurring temperate tree species: the role of positive xylem pressure, wood type and tree stature. Funct Ecol 31:1550–1560.

O'Brien MJ, Leuzinger S, Philipson CD, Tay J, Hector A (2014) Drought survival of tropical tree seedlings enhanced by non-structural carbohydrate levels. Nat Clim Change 4:710–714.

Patino S, Tyree MT, Herre EA (1995) Comparison of hydraulic architecture of woody plants of differing phylogeny and growth form with special reference to freestanding and hemi-epiphytic Ficus species from Panama. New Phytol 129:125–134.

Phillips N, Bergh J, Oren R, Linder S (2001) Effects of nutrition and soil water availability on water use in a Norway spruce stand. Tree Physiol 21:851–860.

Pittermann J, Sperry J (2003) Tracheid diameter is the key trait determining the extent of freezing-induced embolism in conifers. Tree Physiol 23:907–914.

Pivovaroff AL, Santiago LS, Vourlitis GL, Grantz DA, Allen MF (2016) Plant hydraulic responses to long-term dry season nitrogen deposition alter drought tolerance in a Mediterranean-type ecosystem. Oecologia 181:721–731.

Plavcová L, Hacke UG (2012) Phenotypic and developmental plasticity of xylem in hybrid poplar saplings subjected to experimental drought, nitrogen fertilization, and shading. J Exp Bot 63:6481–6491.

Plavcová L, Hacke UG, Almeida-Rodriguez AM, Eryang LI, Douglas CJ (2013) Gene expression patterns underlying changes in xylem structure and function in response to increased nitrogen availability in hybrid poplar. Plant Cell Environ 36:186–199.

Quinn Thomas R, Canham CD, Weathers KC, Goodale CL (2009) Increased tree carbon storage in response to nitrogen deposition in the US. Nat Geosci 3:13.

Sack L, Cowan PD, Jaikumar N, Holbrook NM (2003) The 'hydrology' of leaves: co-ordination of structure and function in temperate woody species. Plant Cell Environ 26:1343–1356.

Sala A, Woodruff DR, Meinzer FC (2012) Carbon dynamics in trees: feast or famine? Tree Physiol 32:764–775.

Salifu KF, Timmer VR (2001) Nutrient retranslocation response of seedlings to nitrogen supply. Soil Sci Soc AM J 65:905–913.

Salleo S, Lo Gullo MA, Trfilo P, Nardini A (2004) New evidence for a role of vessel-associated cells and phloem in the rapid xylem refilling of cavitated stems of Laurus nobilis L. Plant Cell Environ 27:1065–1076.

Salleo S, Trifilò P, Esposito S, Nardini A, Lo Gullo MA (2009) Starch-to-sugar conversion in wood parenchyma of field-growing Laurus nobilis plants: a component of the signal pathway for embolism repair? Funct Plant Biol 36:815–825.

Schulte-Uebbing L, de Vries W (2018) Global-scale impacts of nitrogen deposition on tree carbon sequestration in tropical, temperate, and boreal forests: a meta-analysis. Glob Chang Biol 24:416–431.

Secchi F, Zwieniecki M (2012) Analysis of xylem sap from functional (Nonembolized) and nonfunctional (Embolized) vessels of Populus nigra: chemistry of refilling. Plant Physiol 160:955–964.

Secchi F, Zwieniecki MA (2011) Sensing embolism in xylem vessels: the role of sucrose as a trigger for refilling. Plant Cell Environ 34:514–524.

Spannl S, Homeier J, Bräuning A (2016) Nutrient-induced modifications of wood anatomical traits of Alchornea lojaensis (Euphorbiaceae). Front Earth Sci 4:50.

Sparks JP (2009) Ecological ramifications of the direct foliar uptake of nitrogen. Oecologia 159:1–13.

Sperry JS, Donnelly JR, Tyree MT (1988) A method for measuring hydraulic conductivity and embolism in xylem. Plant Cell Environ 11:35–40.

Tyree MT, Ewers FW (1991) The hydraulic architecture of trees and other woody plants. New Phytol 119:345–360.

Van de Weg MJ, Shaver GR, Salmon VG (2013) Contrasting effects of long term versus short-term nitrogen addition on photosynthesis and respiration in the Arctic. Plant Ecol 214:1273–1286.

Villagra M, Campanello PI, Bucci SJ, Goldstein G (2013) Functional relationships between leaf hydraulics and leaf economic traits in response to nutrient addition in subtropical tree species. Tree Physiol 33:1308–1318.

Wang AY, Han SJ, Zhang JH et al. (2018) The interaction between nonstructural carbohydrate reserves and xylem hydraulics in Korean pine trees across an altitudinal gradient. Tree Physiol 38: 1792–1804.

Wang AY, Wang M, Yang D, Song J, Zhang WW, Han SJ, Hao GY (2016) Responses of hydraulics at the whole-plant level to simulated nitrogen deposition of different levels in Fraxinus mandshurica. Tree Physiol 36:1045–1055.

Xiao L, Liu GB, Li P, Xue S (2017) Nitrogen addition has a stronger effect on stoichiometries of non-structural carbohydrates, nitrogen and phosphorus in Bothriochloa ischaemum than elevated CO2. Plant Growth Regul 83:325–334.

Yang D, Zhang YJ, Song J, Niu C-Y, Hao GY (2018) Compound leaves are associated with high hydraulic conductance and photosynthetic capacity: evidence from trees in Northeast China. Tree Physiol 39:729–739.

Zhang H, Li W, Adams HD et al. (2018) Responses of Woody Plant functional traits to nitrogen addition: a meta-analysis of leaf economics, gas exchange, and hydraulic traits. Front Plant Sci 9:683.

Zhang H, McDowell NG, Adams HD et al. (2019) Divergences in hydraulic conductance and anatomical traits of stems and leaves in three temperate tree species coping with drought, N addition and their interactions. Tree Physiol. doi: 10.1093/treephys/tpz135.

Zhu K, Yuan F, Wang A, Yang H, Guan D, Jin C, Zhang H, Zhang Y, Wu J (2019) Effects of soil rewatering on mesophyll and stomatal conductance and the associated mechanisms involving leaf anatomy and some physiological activities in Manchurian ash and Mongolian oak in the Changbai Mountains. Plant Physiol Bioch 144:22–34.